

# Pyrolysis and combustion model of oil sands from non-isothermal thermogravimetric analysis data

Chunxia Jia · Qing Wang · Jianxin Ge · Xiaofei Xu

Received: 10 July 2013 / Accepted: 9 December 2013 / Published online: 21 January 2014  
© Akadémiai Kiadó, Budapest, Hungary 2014

**Abstract** Thermogravimetric (TG) data of oil sand obtained at Engineering Research Center of Oil Shale Comprehensive Utilization were studied to evaluate the kinetic parameters for Indonesian oil sand samples. Experiments were carried out at heating rates of 5, 15, and 25 °C min<sup>-1</sup> in nitrogen, 10, 20, and 50 °C min<sup>-1</sup> in oxygen atmosphere, respectively. The extent of char combustion was found out by relating TG data for pyrolysis and combustion with the ultimate analysis. Due to distinct behavior of oil shale during pyrolysis, TG curves were divided into three separate events: moisture release, devolatilization, and evolution of fixed carbon/char, where for each event, kinetic parameters, based on Arrhenius theory, were calculated. Coats–Redfern method, Flynn–Wall–Ozawa method, and distributed activation energy model method have been used to determine the activation energies of degradation. The methods are compared with regard to their characteristics and the ease of interpretation of the thermal kinetics. Activation energies of the samples were determined by three different methods and the results are discussed.

**Keywords** Oil sands · Pyrolysis · Combustion · Thermogravimetric analysis

## Introduction

Increasing fuel prices, the eminent fear of the limited conventional energy resources, and the projected growth of

heavy industry have placed great pressure on energy supplies. Oil sand is an abundant resource in USA, Australia, China, Jordan, Morocco, and Estonia and its energy extraction is under intensive research [1]. Oil sand, or tar sand, is bitumen-impregnated sandstone. The sandstone is a packed set of sand grains, and the bitumen resides in the interstices between the grains. Other important components of oil sand are coke and water. Oil sand reserves have only recently been considered to be part of the world's oil reserves, as higher oil prices and new technology enable them to be profitably extracted and upgraded to usable products. There are three methods for oil recovery from oil sand, including hot water extraction, solvent extraction, and retorting. A few of research works on the features of oil sands have been done. The effect of temperature on the viscosity, product yield, and chemical composition of the oil sand bitumen has been reported [2, 3].

High temperature plays an important role in the combustion and gasification of sand oil. Therefore, it is necessary to develop models to predict the behavior of the feedstock when it is subjected to high temperature. The relationship between the extents of reaction as it proceeds with the temperature can be determined by Arrhenius equation. Activation energy ( $E$ ) and pre-exponential factor ( $A$ ) are the two important parameters in Arrhenius equation which are determined by thermal analysis. These parameters can be further used in numerical simulation models such as computational fluid dynamics tools to investigate the behavior of the feedstock under different operating conditions [4].

In addition, thermogravimetric (TG) analysis has been extensively used as a means of determining the kinetic parameters [5–10] of pyrolysis and combustion. In this technique, a sample is weighed continuously as it is heated at a constant rate. The resulting curve of mass change

C. Jia · Q. Wang (✉) · J. Ge · X. Xu  
Engineering Research Center of Oil Shale Comprehensive Utilization, Ministry of Education, Northeast Dianli University, Jilin 132012, Jilin, China  
e-mail: rlx888@126.com

versus time or temperature gives the TG curve. Thermal methods providing information about net results of mass loss and calculation of kinetic parameters are based on simplifying assumptions, which do not correspond to the complex chemical reactions in the thermal degradation of the oil sands. In recent years the application of thermal analysis to study the combustion behavior of crude oils has gained a wide acceptance among researchers. Kök et al. [11–13] investigated thermal characterization and kinetics of Karakus crude oil. In combustion with air, three distinct reaction regions were identified. It was observed that high-temperature oxidation (HTO) activation energy of Karakus crude oil varied between 54.1 and 86.1 kJ mol<sup>-1</sup>, while low-temperature oxidation (LTO) activation energy varied between 6.9 and 8.9 kJ mol<sup>-1</sup>. Sixteen experiments were conducted by Bağcı and Kok [14] to study the combustion reaction kinetics of Turkish crude oils in a limestone medium. The activation energies are almost independent of the gravity of the oil used. The Arrhenius constant is not affected by the API gravity of the oils.

There are a great amount of oil sands in Indonesia. But they own a special feature that it is hard to extract oil from oil sands through hot water or solvent extraction. The most effective way to produce oil is retorting. It has been practiced by Alberta Taciuk Process technology which extracts bitumen from oil sands through retorting. During this process, oil sand is moved through a rotating drum, cracking the bitumen with heat and producing lighter hydrocarbons. Beside the extraction of oil from oil sand, it can also be burnt directly in boiler as a low-grade fuel to provide the electric power and heat for oil sand retort plant. Above all, the research of the thermal characteristics and kinetics of oil sands will be necessary and significant.

In this paper, results on the thermo-oxidative and pyrolysis reactions of Indonesia oil sands are presented. The objective of this research was to investigate the pyrolysis and combustion kinetics of oil sand samples. For this reason three different kinetic models were used and the results were discussed and compared.

## Experimental

In this research, thermogravimetry (TG:DTG) experiments were performed by means of Perkin Elmer Pyris 1 thermal analysis system. The instrument has a wide range of operating conditions from room temperature to 900 °C. In this study, nitrogen was used as the purge gas for thermal cracking reactions, while air was used for oxidation reactions. The flow rate was measured by a volumetric flow meter and was maintained at 80 mL min<sup>-1</sup>. The data analysis system is essentially a built-in computer system. It controls the furnace programming, records the mass change

of the sample against temperature or time, and processes the experimental results.

The two samples were recorded by OS1 and 2. In all cases, the average initial sample mass was about 10 mg, and the particle size was 0–0.2 mm. They were prepared according to the ASTM standards. Table 1 represents the proximate and ultimate analyses of oil sands. It is believed that for such a small particle size the effect of temperature distribution within the sample particle is eliminated. The experiments were performed at three heating rates (5, 15, and 25 °C min<sup>-1</sup> in nitrogen; 10, 20, and 50 °C min<sup>-1</sup> in oxygen atmosphere). It was essential to calibrate and balance for buoyancy effects to allow quantitative estimation of mass changes. The material chosen for investigating such effect was platinum, which has a melting point of 1,773.5 °C. All the experiments were performed twice in order to see the repeatability.

## Results and discussion

### Non-isothermal pyrolysis and oxidation

The pyrolysis TG and the differential TG curves of oil sand at different heating rates are shown in Fig. 1. From the figures, it can be seen that the mass-loss process of oil sand could be divided into three steps: the first step is between 25 and 160 °C, where water volatilizes; the second step is a relatively light organic substance volatilizing and desorbing from 160 to 55 °C, and the third step is between 550 and 810 °C, where the heavy organic substance cracks. The peak temperature represents the maximum rate of mass loss. The reaction intervals, peak and burn-out temperatures, and mass loss for each reaction regions of all samples are given in Table 2.

The heating rate has a strong influence on the shape of a TG curve. The most visible effect is reflected on the procedural decomposition temperatures  $T_i$  and  $T_f$ . For a one-step endothermic decomposition reaction the following is observed: (i)  $(T_f)_h > (T_f)_l$  (ii)  $(T_i)_h > (T_i)_l$  and  $(T_f - T_i)_h > (T_f - T_i)_l$ , where the subscripts h and l denote high and low heating rates, respectively. A sample will begin to decompose when the pressure of the gaseous products exceeds the ambient partial pressure. When the temperature is reached at which this condition is satisfied, decomposition will occur if the product gases can freely diffuse from the sample. In the case of dense packing and/or a high heating rate, such free diffusion is inhibited and the decomposition temperature is increased. At low heating rates the sample temperature is more uniform and diffusion of product gases can occur within the sample, lowering the decomposition temperature. Furthermore, because the sample decomposes in an atmosphere which is more

**Table 1** Proximate and ultimate analysis of oil sands

Samples	Proximate analysis/% (mass content)					Ultimate analysis/%				
	$M_{ar}$	$A_{ar}$	$V_{ar}$	$FC_{ar}$	$Q_{ar.net}/J\ g^{-1}$	$C_{ar}$	$H_{ar}$	$O_{ar}$	$N_{ar}$	$S_{ar}$
OS1	1.30	46.68	52.02	0.00	9,798.50	28.92	2.36	19.22	0.41	1.11
OS2	1.06	48.03	50.91	0.00	9,494.42	28.22	2.79	18.39	0.38	1.13

$M$  moisture,  $A$  ash,  $V$  volatile,  $FC$  fixed carbon,  $ar$  as received basis

**Fig. 1** Non-isothermal pyrolysis TG and DTG curves of oil sand at various heating rates

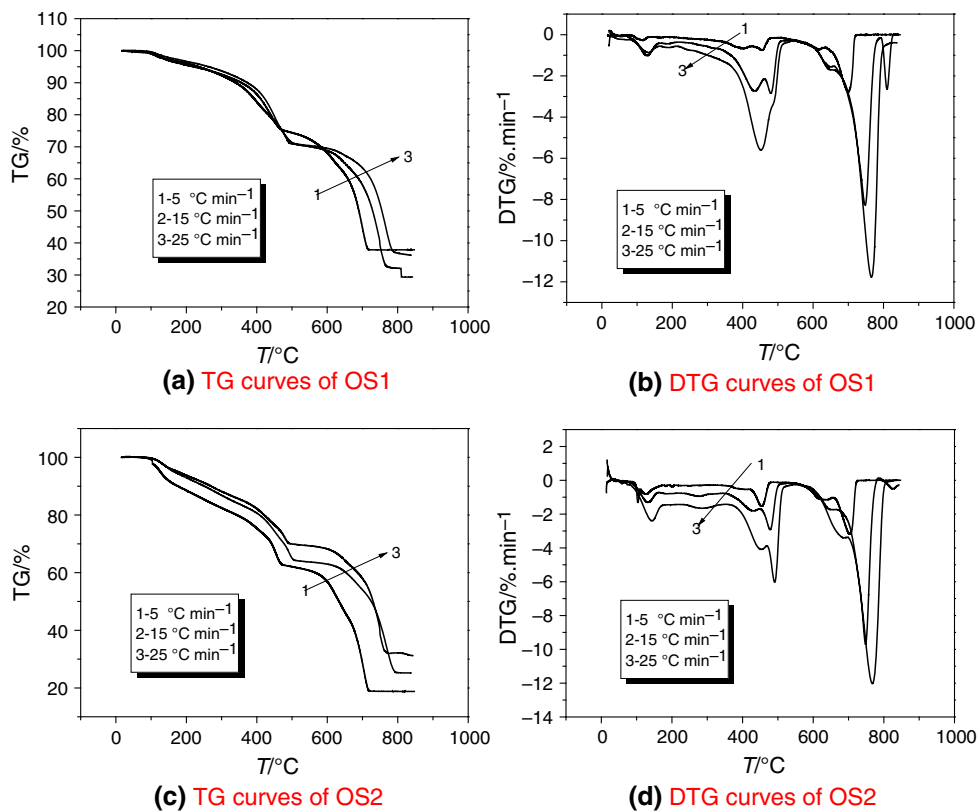
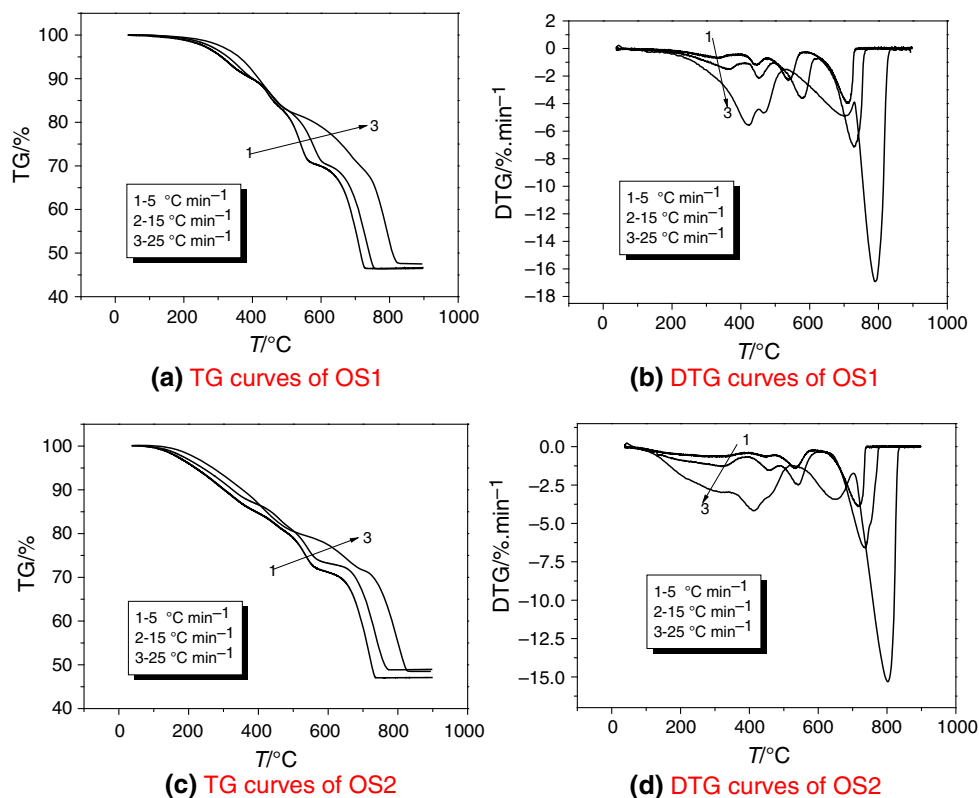


**Table 2** Thermogravimetric characteristics of oil sand at different heating rates

Heating rate/ $^{\circ}C\ min^{-1}$	First region			Second region			Third region			$T_h/^{\circ}C$
	Temperature range/ $^{\circ}C$	Mass loss/%	$T_p/^{\circ}C$	Temperature range/ $^{\circ}C$	Mass loss/%	$T_p/^{\circ}C$	Temperature range/ $^{\circ}C$	Mass loss/%	$T_p/^{\circ}C$	
OS1										
5	25–142	18	113	408–546	17	408	591–800	32	700	800
15	25–170	10	128	408–546	16	434	591–800	31	751	800
25	25–171	11	133	408–546	15	458	591–800	30	761	800
OS2										
5	25–165	10	128	368–551	17	128	543–817	42	705	817
15	25–170	8	137	368–551	19	137	543–817	32	744	817
25	25–182	7	147	368–551	15	147	543–817	44	769	817

$T_p$  peak temperature ( $^{\circ}C$ ),  $T_h$  burn-out temperature

**Fig. 2** Non-isothermal combustion TG and DTG curves of oil sand at various heating rates



constant than at a higher heating rate, the decomposition reaction will be completed within a narrower temperature interval. The disparity between the true sample temperature and the programmed temperature is increased at high heating rates. Also, the extent of sample decomposition is greater at a lower heating rate and where multiple reactions occur the resolution of individual reactions is reduced at high heating rates.

With an increase of the heating rate, the TG curve and peak on the DTG curve shift to a higher temperature region and the final mass loss presents a decreasing trend. The behavior could be explained on the basis of heat transfer and medium diffusion, as reported by others [15]. The mass-loss process happens in a shorter time at a higher heating rate, which makes the part of a relatively light organic substance volatilize at a higher temperature, which should volatilize at a lower temperature, so that the DTG curve shifts to a higher temperature region and the final mass-loss decreases.

The combustion TG/DTG curves of the oil sands at various heating rates are shown in Fig. 2. The mass loss observed in the oil sands was assumed to represent the thermal decomposition of the indigenous bitumen. The DTG curves revealed that reactions occurred at three different stages in all the samples. The differences noticed in the TG characteristic values of the two samples, especially in terms of mass loss are due to the difference in the origin of the bitumen. The first reaction occurred between 25 and

335 °C, called the low-temperature oxidation (LTO). Light hydrocarbons evolved during the thermal decomposition were oxidized in this region [16, 17]. The second transition took place between 335 and 480 °C called the fuel deposition according to the classification of Kok and Gundogar [18]. The observed mass loss in this region was due to the combination of hydrocarbon combustion and thermal cracking reactions which compete with each other [9]. Carbon-rich residue (coke) was formed at this stage and deposited as fuel. The final reaction which involved the combustion of the remaining hydrocarbons and carbon residue occurred between 480 and 540 °C and is called the HTO. The oil sands have lower peak temperatures in comparison with the bitumen extracts.

#### Non-isothermal kinetic models

Non-isothermal kinetic study of mass loss under pyrolysis and combustion processes is extremely complex for oil sands because of the presence of numerous complex components and their parallel and consecutive reactions. In the course of this research, three different models [C–R (Coats–Redfern), F–W–O (Flynn–Wall–Ozawa), and DAEM (distributed activation energy model)] all based on Arrhenius kinetic theory were used for kinetic analysis of the data generated by the TG experiments.

The calculation of the kinetic data is based on the formal kinetic equation:

**Fig. 3** The  $\alpha$ - $T$  curves of oil sand samples at various heating rates (pyrolysis)

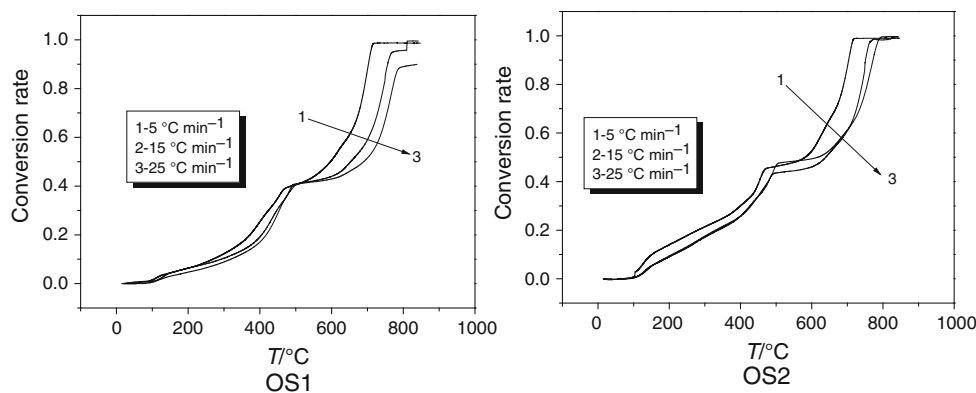
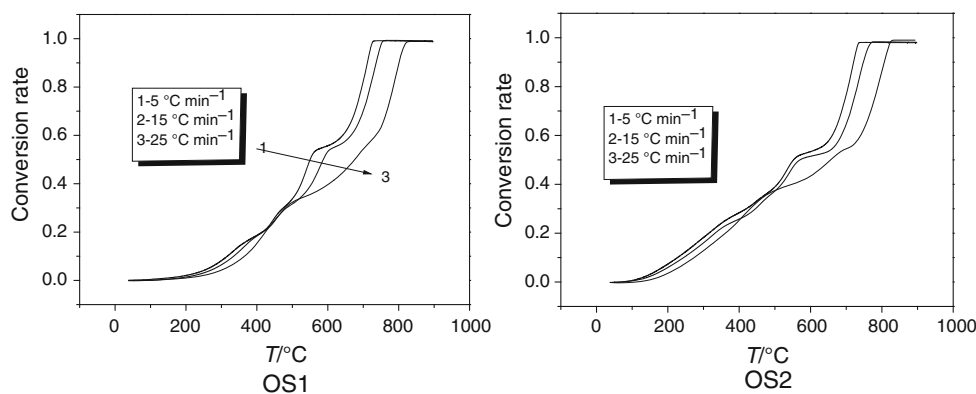


**Fig. 4** The  $\alpha$ - $T$  curves of oil sand samples at various heating rates (combustion)



$$\frac{d\alpha}{dT} = \frac{1}{\beta} k(T) f(\alpha) \tag{1}$$

where  $\alpha$  is fraction of conversion,  $n$  is the order of reaction,  $k$  is the specific rate constant, and  $f(\alpha)$  is the kinetic mechanism.

The temperature dependence of  $k(T)$  is expressed by the Arrhenius equation:

$$k = A \exp\left(-\frac{E}{RT}\right) \tag{2}$$

where  $A$  is the pre-exponential factor;  $E$  is the activation energy;  $T$  is the temperature; and  $R$  is the universal gas constant,  $8.314 \text{ J mol}^{-1} \text{ K}^{-1}$ .

The integration of Eq. (1) results is:

$$\frac{d\alpha}{dT} = \frac{A}{\beta} \exp\left(-\frac{E}{RT}\right) f(\alpha) \tag{3}$$

According to the TG curves, the relationship of the reaction conversion rate and temperature of oil sand samples are depicted in Figs. 3 and 4. From these figures, similar trends at the different heating rate occurred and the conversion rate gradually increases with the rising of temperature. The change of conversion rate is less striking at low temperature and high temperature, but the change is pronounced at the medium temperature.

*C-R method*

This method uses a single heating rate and various conversion functions and gives idea about the degradation mechanism along with the activation energy ( $E$ ) and the pre-exponential factor ( $A$ ) values. It is based on the following equation [19]:

$$\ln\left\{\frac{1 - (1 - \alpha)^{1-n}}{T^2(1 - n)}\right\} = \ln\left\{\frac{AR}{\beta E} \left[1 - \frac{2RT}{E}\right]\right\} - \frac{E}{RT} \quad n \neq 1 \tag{4}$$

$$\ln\left[\frac{-\ln(1 - \alpha)}{T^2}\right] = \ln\left\{\frac{AR}{\beta E} \left[1 - \frac{2RT}{E}\right]\right\} - \frac{E}{RT} \quad n = 1 \tag{5}$$

$g(a)$  can be obtained from the following equation:

$$g(a) = -\ln(1 - a) \text{ or } g(a) = 1 - \ln(1 - a)^{(1-n)} \tag{6}$$

The curve  $\ln[g(a)/T^2]$  versus  $1/T$ , obtained from TG curves recorded at a single heating rate, yields a straight line whose slope and intercept allows the evaluation of activation energy and pre-exponential factor, respectively. Also, the best fitting model of conversion degradation function  $[g(a)]$  gives the probable mechanism for the degradation of the samples.

### F–W–O analysis

$$\lg \beta = \lg \left( \frac{AE}{RG(\alpha)} \right) - 2.315 - 0.4567 \frac{E}{RT} \quad (7)$$

This is an iso-conversional integral method [20, 21] obtained from TG curves recorded at several heating rates yields a straight line whose slope allows evaluation of the activation energy.

### DAEM

The DAEM has been widely used to analyze complex reactions, such as combustion of fossil fuels. The model, originally proposed by Vand [22], assumes a number of irreversible first-order parallel reactions with different activation energy  $E$  values to occur simultaneously, where the difference in activation energies is represented by a distribution function  $f(E)$ . Miura et al. [22] have recently proposed two methods to estimate  $f(E)$  and  $k_0(E)$ , a differential method and an integral method, from a set of three TG experiments at different heating rates without assuming  $k_0$  value and functional form for  $f(E)$ . Although both methods are the same in principle, the integral method is more accurate and does not need a tedious differentiation step. When the model is used to analyze oil sands combustion, change in the total volatiles,  $V$ , against time,  $t$ , is given by

$$1 - V/V^* = \int_0^\infty \exp \left( -k_0 \int_0^t e^{-E/RT} dt \right) f(E) dE \quad (8)$$

where  $V^*$  is the effective volatile content of the oil sands,  $f(E)$  is the normalized distribution curve of the activation energy, and  $k_0$  is the frequency factor corresponding to the  $E$  value. Eq. (6) was simplified to Eq. (7) by Miura [23].

$$V/V^* = 1 - \int_{E_s}^\infty f(E) dE = \int_0^{E_s} f(E) dE \quad (9)$$

In this simplified model, the Arrhenius equation can be described as follows:

$$\ln \left( \frac{\beta}{T^2} \right) = \ln \left( \frac{k_0 R}{E} \right) + 0.6075 - \frac{E}{RT} \quad (10)$$

Using Eq. (8), we can estimate both  $E$  and  $k_0$  from the Arrhenius plot of  $\ln(\beta/T^2)$  versus  $1/T$  at the selected  $V/V^*$  values for different  $a$  values. The relationship between  $V/V^*$  versus  $E$  could be obtained by plotting the  $V/V^*$  value against the corresponding  $E$  value. No assumptions are required for the functional forms of  $f(E)$  and  $k_0(E)$  [23].

**Table 3** Pyrolysis kinetic parameters of oil sand samples by C–R method

Sample	Heating rate/ °C min <sup>-1</sup>	$R^2/^\circ\text{C}$	$E/\times 10^3 \text{ J mol}^{-1}$	$A/\text{min}^{-1}$
OS1	5	0.98980	104.1335	628.33
	15	0.99118	116.4332	8,758.93
	25	0.99434	144.0880	851.58
OS2	5	0.98645	110.4019	388.01
	15	0.98061	111.9380	2,198.78
	25	0.97954	117.2653	3,127.60

### Pyrolysis kinetic results

#### C–R analysis result

Figure 3 shows the typical plot of  $\ln[-\ln(1 - a)/T^2]$  versus  $1/T$ , indicating that the reaction of oil sand pyrolysis could be described by  $n = 0.5$  reaction in the studied temperature region. From the slope and intercept of the line, the values of  $E$  and  $A$  can be obtained. Table 3 shows the kinetic parameters of oil sand pyrolysis at different heating rates that were determined by C–R method. As can be seen, all correlation coefficients are larger than 0.989, which indicates that the first-order reaction model fits the experimental data very well. The heating rate has some effect on the activation energy and pre-exponential factor. For OS1, the activation energy and pre-exponential factor increase from  $104 \times 10^3$  and 628 to  $144 \times 10^3 \text{ J mol}^{-1}$  and 3,127 with the increase of the heating rate from 5 to 25 °C min<sup>-1</sup>, respectively. This is assigned to the combined effects of the heat transfer at different heating rates and kinetics of the decomposition, resulting in the delayed effects of the decomposition.

#### DAEM and F–W–O analysis results

According to Eq. (1), a plot of  $\ln(\beta/T^2)$  (or  $\lg \beta$ ) versus  $1/T$  was performed to obtain activation energy  $E$  at each selected level of conversion rate. The apparent activation energy can be evaluated from the slope of these fitting straight lines. Figure 5 illustrates that the correlation of the regression lines is very good and the magnitude of correlation coefficient exceeds 0.99. At the same time, it is discovered that the fitting lines at the different conversion rates are parallel to one another ( $a = 0.05, 0.1, 0.15, \dots, 0.95$ ), then the relationship between  $E$  versus  $a$  could be obtained, Fig. 6 illustrates the variations of the activation energy of the two oil sand samples with the conversion rate.

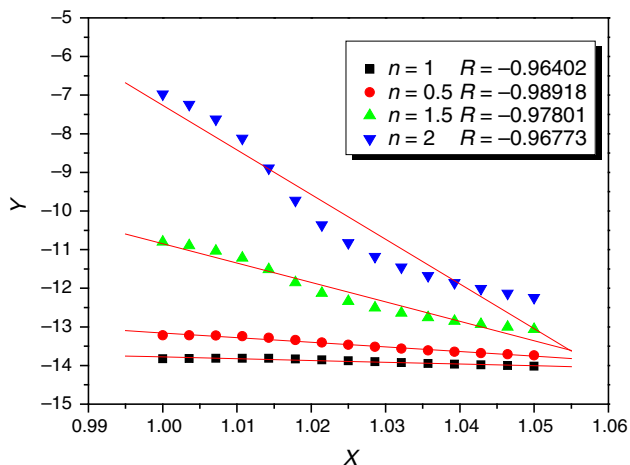


**Fig. 5** Analysis of oil sand pyrolysis by Coats–Redfern method ( $Y = \ln(-\ln(1 - a)/T^2)$ ,  $X = 1/T$ )

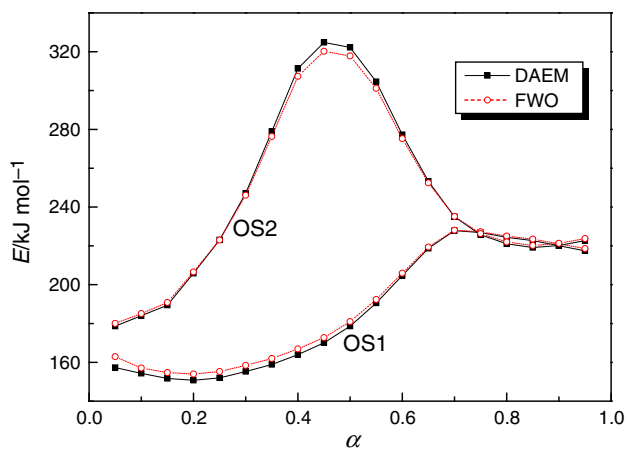


**Fig. 6** The  $E-\alpha$  curves of oil sand pyrolysis analyzed by DAEM and F–W–O method

The activation energies calculated by two methods are much closer. The results vary greatly for different oil sands, and the average activation energy of OS1 is much smaller than OS2, because the oil sands have different physical and chemical properties.

The plots of pyrolysis  $E-\alpha$  of oil sand samples analyzed by DAEM and F–W–O method are shown in Fig. 6. The figure illustrates that, for each sample, apparent activation energy  $E$  at the whole temperature region is not constant, increasing at first then following a decreasing trend; for all samples, the differences in composition of oil sands cause the different values of  $E$ . For instance, the higher volatile content of OS1 led to the smaller  $E$ , because the higher volatile content endows the reaction easier to take place. Besides, the values of  $E$  are all approaching approximately  $220 \times 10^3 \text{ J mol}^{-1}$ , which means that thermal decomposition of indigenous bitumen comes to an end around certain value.

From the distribution point of  $E-a$ , the activation energy is not constant, the fluctuation range is large, and activation energy of OS1 decreases at first and then slowly rises during the pyrolysis reaction process, because the escaping rate of generated volatile increases with the rise of temperature, the activation energy exhibits a reduced tendency, i.e., from the initial  $150 \times 10^3 \text{ J mol}^{-1}$  increases to about  $228 \times 10^3 \text{ J mol}^{-1}$  in the conversion rate reached 0.7, finally it has become smooth; for OS2, the activation energy peak appeared in the intermediate segment of thermal cracking reaction, it is from the initial  $180 \times 10^3 \text{ J mol}^{-1}$  up to  $320 \times 10^3 \text{ J mol}^{-1}$ , eventually fell to  $220 \times 10^3 \text{ J mol}^{-1}$ , it is rising sharply and rapidly declining. The activation energy values of two kinds of samples both tend to be approximately  $220 \times 10^3 \text{ J mol}^{-1}$  in the pyrolysis process, which showed that the oil sands' high degree thermal cracking reaction came to an end.

Combustion kinetic results

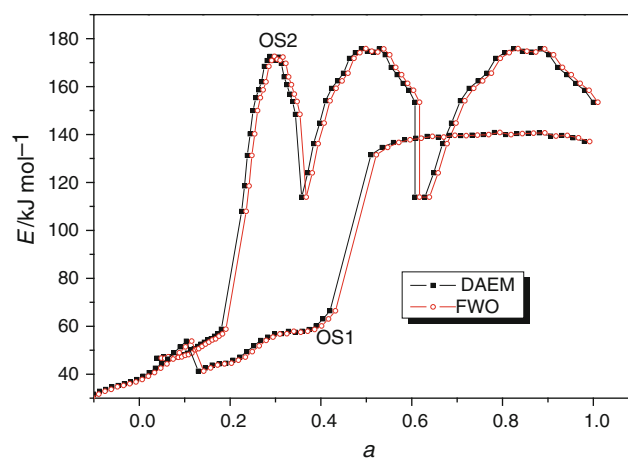
C–R analysis

The combustion kinetic parameters of oil sands are shown in Table 4. As can be seen, in different reaction phases, the apparent activation energy and reaction order are variable. Non-isothermal kinetic study of mass loss under combustion process is extremely complex for oil sands because of the presence of the numerous complex components and their parallel and consecutive reactions. Within the analysis it was observed that all the oil and samples have more than one reaction zone so that kinetic parameters were calculated for three reaction regions. The first reaction region is known as LTO, the second one is medium-temperature oxidation zone, and the third one is HTO zone (Fig. 2). Throughout the kinetic analysis, it was observed that the first zone's activation energies were generally lower than those of the second one (Table 3), and the third zone's activation energies were the maximum value, because organic compounds mostly decomposed at higher temperatures than other mineral-type compounds. The pre-exponential factor of OS2 presents the same changing trend as the activation energy; but for OS1, the second reaction region's pre-exponential factors are the maximum values. The results show that different oil sand samples have different combustion characteristics.

From Table 4, it was found that for various heating rates there were insignificant variations in the kinetic parameters. The apparent activation energy values for the LTO and HTO reactions varied from 62 to 80 and 354 to  $381 \times 10^3 \text{ J mol}^{-1}$  for OS1 and from 65 to 78 and 326 to  $346 \times 10^3 \text{ J mol}^{-1}$  for OS2, respectively. This result suggests a catalytic effect of sand on the oxidative reactions taking place during the thermal decomposition of the

**Table 4** The combustion kinetic parameters of oil sands

Sample	Heating rate/ $^{\circ}\text{C min}^{-1}$	First stage			Second stage			Third stage					
		$E/\times 10^3 \text{ J mol}^{-1}$	$r$	$n$	$E/\times 10^3 \text{ J mol}^{-1}$	$r$	$n$	$E/\times 10^3 \text{ J mol}^{-1}$	$r$	$n$			
OS1	10	62	1.5	1	39	1.5	1	257	0.99	1	354	0.98	1
	20	78	1.5	1	52	1.5	1	264	0.98	1	367	0.98	1
	50	80	1.5	1	37	1.5	1	282	0.98	1	381	0.98	1
OS2	10	65	0.98	1.5	1.256	0.98	1.5	152	0.99	1	326	0.97	1.5
	20	86	0.98	1.5	3.968	0.98	1.5	162	0.98	1	341	0.97	1.5
	50	78	0.98	1.5	5.326	0.98	1.5	173	0.99	1	346	0.99	1.5

**Fig. 7** The  $E-\alpha$  curves of oil sand combustion analyzed by DAEM and F-W-O method

bitumen contained in the oil sand. Some other researchers have found that kinetic parameters were influenced by many factors, such as the type of oil sands, the temperature interval for calculation, the mathematics analysis methods, the type of pyrolysis, and so on. So there was a wide variation in the literatures for values of kinetic parameters.

#### DAEM and F-W-O analysis

Using the conversion rate  $\alpha$  and temperature values from the TG data, a plot of  $\ln\{-\ln/T^2\}$  versus  $1/T$  should result in a straight line. Arrhenius constant,  $A$ , and activation energy,  $E$ , can be obtained from the intercept and slope of the line. The oil sand OS2 has lower activation energy and Arrhenius constant values in comparison with OS1 (Table 3).

The apparent activation energy changing trends analyzed by DAEM method and F-W-O method are basically similar. But they are significantly different from the results calculated by C-R method. The curves of activation energy with the conversion rate in the whole oxidization reaction are shown in Fig. 7; as can be seen, the oil sand burning is instantaneous during the whole combustion process, the apparent activation energies are constantly changing as the reaction proceeds. Although the C-R analysis results also reflect the combustion process of segmentation, and different series of reaction equations have been used to illustrate combustion characterization of oil sands at different stages, the activation energy value of C-R method is only the average of one stage which cannot reflect the transient combustion reaction.

It can be seen that activation energies of two oil sands show similar changing trend, first it increases with the rise of the conversion rate and then decreases slowly, The activation energy values varied from  $50 \times 10^3$  to



$90 \times 10^3 \text{ J mol}^{-1}$  until conversion rate is 0.3, then it changing slowly; the activation energy of OS2 can maintained in  $80 \times 10^3 \text{ J mol}^{-1}$ . When conversion rate is greater than 0.6, apparent activation energy increase again with the rise in conversion rates, the sample OS1 increases to  $200 \times 10^3 \text{ J mol}^{-1}$ , OS2 increased to about  $160 \times 10^3 \text{ J mol}^{-1}$ . Apparently the activation energy of late phase is much larger compared with the former two phase activation energy.

The curve of  $\ln(A) \sim E$  was received, the salient point of compensation effect can be seen in the figure, which corresponds to the change of the activation energy, and the results will be provided in detail later.

## Conclusions

In the course of this research, an experimental study on the thermal characteristics and kinetic parameters of the Indonesian oil sand sample was presented. The experiment was conducted at non-isothermal heating conditions both in nitrogen and oxygen atmospheres. The pyrolysis and combustion mass-loss process of oil sand could be divided into different stages in all the samples. Kinetic parameters (both pyrolysis and combustion) of oil sand samples were determined using three different methods (C–R, F–W–O, and DAEM). The results show that the apparent activation energy change trends analyzed by DAEM method and F–W–O method are basically similar. But they are significantly different from the results calculated by C–R method. Although the C–R analysis results also reflect the oil combustion process of segmentation and different series reaction equations have been used to illustrate combustion and pyrolysis characterization of oil sands at different stages, but the activation energy value of C–R method is only the average of one stage which cannot reflect the transient combustion reaction.

**Foundation item** Natural Science Foundation of China (51276034).

## References

- Meng M. Extraction of organic substance from Tumuji oil sand. Dalian: Dalian University of Technology; 2007.
- Dai Q, Chung KH. Hot water extraction process mechanism using model oil sands. *Fuel*. 1996;75:220–6.
- Liu Q, Cui Z, Etsell TH. Characterization of Athabasca oil sands froth treatment tailings for heavy mineral recovery. *Fuel*. 2006;85:807–14.
- Philips CR, Lymes R, Halahel TM. Enthalpies of pyrolysis and oxidation of Athabasca oil sands. *Fuel*. 1982;61:639–46.
- Wang XB, Si JP, Tan HZH. Kinetics investigation on the combustion of waste capsicum stalks in Western China using thermogravimetric analysis. *J Therm Anal Calorim*. 2012;109:403–12.
- Mehta SK, Kaur R, Singh S. Thermogravimetric evaluation of decomposition kinetics of metal surfactant complexes. *J Therm Anal Calorim*. 2012;107:69–75.
- Sasmal S, Goud VV, Mohanty K. Determination of salutary parameters to facilitate bio-energy production from three uncommon biomasses using thermogravimetric analysis. *J Therm Anal Calorim*. 2013;111:1649–55.
- Luo MY, Xia DH, Liu WD, Liu XG. A study on the thermogravimetric characters of oil sands and its application to thermal oil extracting system. *Boil Manuf*. 2007;1:73–6.
- Sonibare OO, Egashira R, Adedosu TA. Thermo-oxidative reactions of Nigerian oil sand bitumen. *Thermochim Acta*. 2003;405:195–205.
- Wang Q, Jia CX, Jiang QQ, Wang Y. Combustion characteristics of Indonesian oil sands. *Process Technol*. 2012;99:110–4.
- Kök MV, Acar C. Kinetics of crude oil combustion. *J Therm Anal Calorim*. 2006;83(2):445–9.
- Kök MV. Non-isothermal kinetic analysis and feasibility study of medium grade crude oil field. *J Therm Anal Calorim*. 2008;91(3):745–8.
- Kök MV, Pokol G, Keskin C. Light crude oil combustion in the presence of limestone matrix. *J Therm Anal Calorim*. 2004;75:781–6.
- Bagcı S, Kok MV. Combustion reaction kinetics studies of Turkish crude oils. *Energy Fuels*. 2004;18:1472–81.
- Meng M, Hu HQ, Zhang QM, Li X, Wu B. Pyrolysis behaviors of Tumuji oil sand by thermogravimetry (TG) and in a fixed bed reactor. *Energy Fuels*. 2007;21(4):2245–9.
- Kok MV. Characterization of medium and heavy crude oils using thermal analysis technique. *Fuel Process Technol*. 2011;92:1026–31.
- Nader M, Thiakavathi M. Thermal cracking and combustion kinetics of asphaltene derived from Fosteron oil. *Fuel Process Technol*. 2009;90(10):1286–91.
- Kok MV, Gundogar EAS. Effect of different clay concentrations on crude oil combustion kinetics by thermogravimetry. *Therm Anal Calorim*. 2010;99:779–83.
- Sonibare R, Egashira TA, Adedosu. Thermo-oxidative reactions of Nigerian oil sand bitumen. *Thermochim Acta*. 2003;405:195–205.
- Coats AW, Redfern JP. Kinetic parameter from thermo-gravimetric data. *Nature*. 1964;20:489–93.
- Hu RZ. Kinetics of thermal analysis. Beijing: Science Press; 2001. p. 57–9.
- Vand V. A theory of the irreversible electrical resistance changes of metallic films evaporated in vacuum. *Proc Phys Soc Lond*. 1943;5:222–46.
- Miura K. A new and simple method to estimate  $f(E)$  and  $k_o(E)$  in the distributed activation energy model from three sets of experimental data. *Energy Fuels*. 1995;9:302–7.